

Influence of Modified Oxide Inclusions on Initiation of Rolling Contact Fatigue Cracks in Bearing Steel

Masaki SHIMAMOTO*¹, Dr. Eiichi TAMURA*¹, Akihiro OWAKI*², Akihiro MATSUGASAKO*²

¹Material Research Laboratory, Technical Development Group

²Wire Rod & Bar Products Development Department, Research & Development Laboratory, Iron & Steel Business

In order to elucidate the mechanism by which the modification of oxide inclusions in bearing steel leads to the improvement of rolling contact fatigue (RCF) properties, a study was conducted with particular attention to the difference in the crack initiation time. Compared with normal Al-killed steel, non-Al-killed steel with modified oxide inclusions has been confirmed to exhibit improved rolling contact fatigue properties. Investigations using ultrasonic testing (UT) and acoustic emission (AE) have revealed that the non-Al-killed steel has a smaller number of defects detected by UT and the number of signals detected by AE, both indicating the suppressed initiation of initial cracks. A study done on the reasons shows that SiO₂-based inclusions generated in the non-Al-killed steel have excellent adhesion between each inclusion and the matrix, with a smaller difference in Young's modulus between them. Therefore, it is conceivable that the non-Al-killed steel experiences a decreased amount of the strain change that occurs in the vicinity of inclusions during rolling load, which suppresses the initiation of initial cracks and improves the rolling contact fatigue properties.

Introduction

Bearing parts are used in various industrial machines and automobiles and require high reliability. Hence, excellent rolling contact fatigue properties are required for the bearing steel used in bearing parts, and various researches have been conducted focusing on non-metallic inclusions (hereinafter referred to as "inclusions"), which can become the origin of fatigue fracture.

As a result of previous studies, flaking due to rolling contact fatigue originated from inclusions is considered to occur through the following process:¹⁾

- (1) Initiation of cracks from inclusions as points of origin.
- (2) Steady propagation of cracks.
- (3) Flaking due to the rapid propagation of cracks.

Of these cracks, those that are initiated from inclusions as points of origin are considered to occur very early in rolling contact fatigue. Udagawa et al.²⁾ reported that the initiation time of cracks from oxide inclusions as the points of origin is 1×10^4 cycles.

Tsuchida et al.³⁾ discussed the initiation mechanism of cracks from inclusions as the points of origin. They clarified that not only the size of

the inclusions but also the Young's modulus of the inclusions and the adhesion state of the interface between the inclusions and the matrix must be considered for the initiation of cracks.

Hashimoto et al.⁴⁾ prepared normal Al-killed steel and another kind of steel made by a modified deoxidation method and observed the characteristics of the interface between the inclusions and matrix. According to their report, there are gaps in the periphery of each Al₂O₃ inclusion in the normal Al-killed steel, whereas Al₂O₃ · SiO₂ based inclusions in the steel produced by the modified deoxidation method adhere well with the matrix, and the steel prepared by the modified method has a longer life.

However, it has not been clarified how modifying the oxide inclusions by changing the deoxidation method makes a difference in the crack initiation time.

Hence, Kobe Steel focused particularly on the difference in crack initiation time, with the aim of elucidating the mechanism through which rolling contact fatigue properties are improved by modifying oxide inclusions, a type of inclusion. Also, the reason for the difference in crack initiation time was discussed from the viewpoints of inclusion size, adhesion between the inclusions and matrix, and Young's modulus of inclusions, which are considered to be factors affecting crack initiation.

1. Experimental method

Samples AL-1 and AL-2 were prepared as normal Al-killed steel. In addition, samples Non-AL-1 and Non-AL-2 were prepared as non-Al-killed steel to modify oxide inclusions. **Table 1** shows the chemical compositions of the samples. AL-1, Non-AL-1, and Non-AL-2 were melted in an induction melting furnace (melting capacity: 170 kg), and then hot-forged and hot-rolled into material with a diameter of 65 mm. A billet produced in the actual process was used to prepare AL-2, which was hot-rolled into material with a diameter of 65 mm. Each hot-rolled material was cut, spheroidizing annealed (795°C × 6 h), quenched (840°C × 30 min), tempered (160°C × 2 h), and final polished into specimens for a thrust-type rolling contact fatigue test.

Thrust-type rolling contact fatigue tests were conducted on AL-1 and Non-AL-1 under the

Table 1 Chemical compositions and deoxidation type of steel samples^{5), 6)}

No.	Deoxidation type	C	Si	Mn	Cr	Al	P	S	O
		wt%	wt%	wt%	wt%	wt%	wt%	wt%	ppm
AL-1	Al-killed	1.08	0.25	0.36	1.47	0.017	0.013	0.005	4
AL-2	Al-killed	1.00	0.25	0.31	1.47	0.022	0.011	0.005	3
Non AL-1	Non Al-killed	1.01	0.25	0.35	1.47	<0.001	0.016	0.001	16
Non AL-2	Non Al-killed	1.02	0.25	0.35	1.47	0.001	0.014	0.001	13

Table 2 Conditions of thrust-type rolling contact fatigue test^{5), 6)}

Ball diameter	9.53 mm(SUJ2)
Number of balls	3
Contact surface pressure	5.24 GPa
Rolling contact frequency	1,500 rpm
Number of specimens	16
Maximum number of cycles	2×10^8

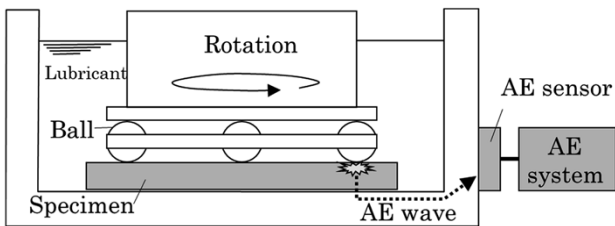


Fig. 1 Schematic diagram of thrust-type rolling contact fatigue test and AE sensor

conditions shown in **Table 2** to investigate the effect of modified oxide inclusions on the rolling contact fatigue properties. Also, in order to investigate how the modification of oxide inclusions affects the crack initiation time, thrust-type rolling contact fatigue tests were conducted on AL-2 and Non-AL-2 under the conditions in Table 2. AL-2 and Non-AL-2 were subjected to ultrasonic testing (hereinafter referred to as "UT") during the rolling contact fatigue test. The UT was performed under a frequency of 125 MHz, and the conditions were adjusted such that the specimen surface layer of 0.05 to 0.45 mm thick fell within the detection range. The entire surface of each specimen was regarded as the observation surface for UT, and the number of defects immediately below the transfer surface of each steel sphere was examined.

Furthermore, in order to investigate the crack initiation time and propagation status as needed, an acoustic emission (hereinafter referred to as "AE") apparatus was installed in the specimen holder of the thrust-type rolling contact fatigue test machine (**Fig. 1**) to detect AE signals emitted from inside the specimens during the rolling contact fatigue test.

2. Experimental results

2.1 Properties of thrust-type rolling contact fatigue

Fig. 2 shows the results of rolling contact fatigue tests. The non-Al-killed steel (Non-AL-1) has an L_{10} life^{Note)} of 2.0×10^8 cycles or higher, an improvement compared with the 6.1×10^6 cycles of the Al-killed steel (AL-1). Thus, the rolling contact fatigue properties have been improved by changing the deoxidation method. It should be noted that none of the Non-AL-1 specimens exhibited flaking, and the test was aborted at a load count of 2.0×10^8 cycles.

2.2 Crack initiation time (UT, AE evaluations)

The Al-killed steel (AL-2) was evaluated by UT at the initial stage of the rolling contact fatigue test (load count, 1.0×10^6 cycles). As a result, 20 defects were detected immediately below the rolling contact surface (**Fig. 3 (a)**). In addition, as the load count increased, the number of defects detected by UT increased (**Fig. 3 (b)**, load count 6.3×10^6 cycles). It should be noted that flaking occurred in the AL-2 specimen at the load count of 6.3×10^6 cycles, and the test was aborted.

On the other hand, in the case of the non-Al-

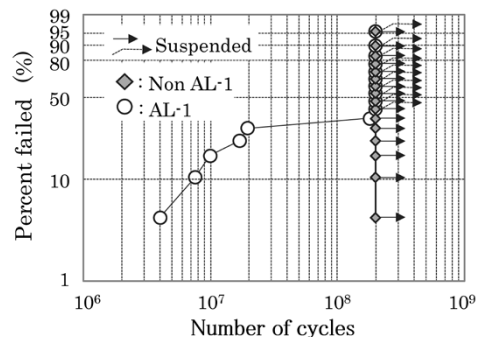


Fig. 2 Results of thrust-type rolling contact fatigue test on AL-1 and Non-AL-1⁵⁾

Note) Number of load cycles with a cumulative failure probability of 10%

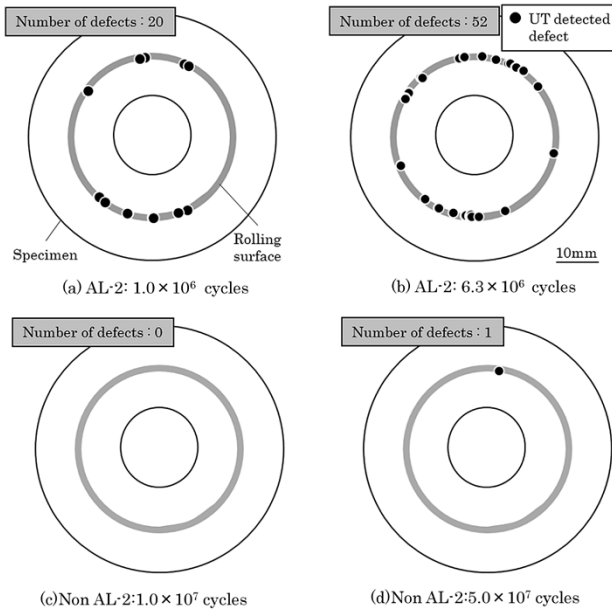


Fig. 3 UT test results of rolling contact fatigue test specimens⁶⁾

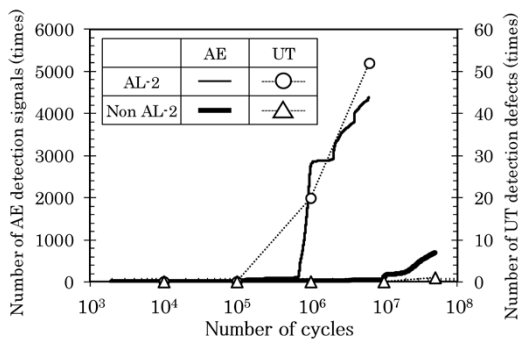


Fig. 4 Relationship between rolling contact fatigue cycles and number of AE signals and UT defects⁶⁾

killed steel (Non-AL-2), no defects were detected by UT at the load count of 1×10^7 cycles (Fig. 3 (c)), and one defect was detected by the same at the load count of 5×10^7 (Fig. 3 (d)).

Next, Fig. 4 shows the changes in the number of signals detected by AE. For the Al-killed steel (AL-2), the total number of AE signals exceeded 100 at the load count of 5.7×10^5 cycles, whereas, for the non-Al-killed steel (Non-AL-2), the total number of AE signals exceeded 100 at the load count of 1.0×10^7 cycles. Fig. 4 also shows the transition of the number of defects detected by UT, and it was found that the non-Al-killed steel (Non-AL-2) had fewer AE signals and UT defects than the Al-killed steel (AL-2), and the time of detection was late in each case.

3. Effect of modifying oxide inclusions on crack initiation time

As described in Section 2, the non-Al-killed steel with modified oxide inclusions has improved rolling

contact fatigue properties compared with the normal Al-killed steel. The results of UT and AE evaluations indicate that the Al-killed steel shows an increase in the number of UT defects and the number of AE signals in the initial stage of the rolling contact fatigue test. On the other hand, the non-Al-killed steel had fewer UT defects and AE signals, and the time of detection was also late in each case. From these results, cracks initiated from oxide inclusions are considered to be suppressed in the non-Al-killed steel. This has led to tests and discussions as to the reasons why the modification of oxide inclusions causes a difference in crack initiation time.

3.1 Modification of inclusions

In order to confirm the modification of inclusions brought about by the change in deoxidation method, the inclusion before the thrust-type rolling contact fatigue test was observed with a scanning electron microscope (SEM) (Fig. 5). Inclusion compositions were analyzed using energy dispersive X-ray spectroscopy (EDS), and, as a result, complex inclusions consisting of Al_2O_3 -base inclusions and MnS were observed in the Al-killed steel (AL-1). On the other hand, in the non-Al-killed steel (Non-AL-1), no Al_2O_3 -based inclusions were observed, but SiO_2 -based inclusions were.

3.2 Inclusion size

The effect of inclusion size was investigated, as it is considered to be a factor affecting the initiation of cracks. The inclusion size is expressed by the following equation:

$$\sqrt{a \times b} \dots \dots \dots (1),$$

wherein a (μm) is the minor axis diameter of an inclusion, and b (μm) is the major axis diameter of the inclusion. The maximum sizes of the inclusions in the Al-killed steel (AL-1) and non-Al-killed steel (Non-AL-1) were predicted by extreme value statistics.

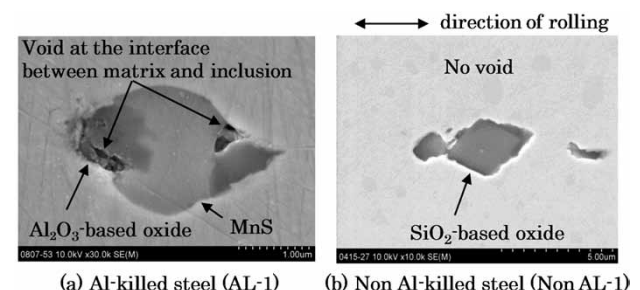


Fig. 5 SEM observation results of non-metallic inclusion before rolling contact fatigue test⁵⁾

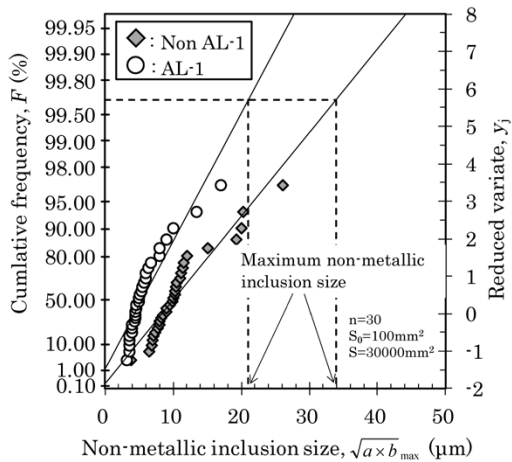


Fig. 6 Predicted maximum size of non-metallic inclusions in AL-1 and Non-AL-1

The analysis results are shown in Fig. 6. The vertical axes of the graph represent cumulative distribution function F and standardized variable y_j . The maximum inclusion size for the Al-killed steel (AL-1) was $21.0\ \mu\text{m}$ and that for the non-Al-killed steel (Non-AL-1) was $33.9\ \mu\text{m}$.

The inclusion size for the Al-killed steel is smaller than that for the non-Al-killed steel, thus inclusion size cannot explain why crack initiation was suppressed in the non-Al-killed steel.

3.3 Adhesion between inclusions and matrix

The adhesion between inclusions and matrix was investigated. As shown in Fig. 5, gaps were observed at the interface between inclusion and matrix in the Al-killed steel (AL-1). The gaps exist at both ends of each inclusion and lie in the hot rolling direction. On the other hand, in the non-Al-killed steel (Non-AL-1), no gap was observed at the inclusion-matrix interface nor in the SiO_2 -based inclusions.

In other words, the modified inclusions in the non-Al-killed steel were found to adhere better to the matrix than the inclusions generated in the Al-killed steel.

3.4 Young's modulus of inclusions

The Young's moduli of inclusions were investigated. In the case of the Al-killed steel, the Young's modulus of Al_2O_3 generated as Al_2O_3 -based inclusions is approximately 380 GPa.⁷⁾ The Young's modulus of MnS generated at the same time is reported to be 137 GPa, and the Young's modulus of matrix is reported to be 206 GPa⁸⁾. The difference $\Delta E (E_{\text{Matrix}} - E_{\text{Inclusion}})$ between the Young's modulus of the matrix, E_{Matrix} , and the Young's modulus of an inclusion, $E_{\text{Inclusion}}$, is approximately -174 GPa for

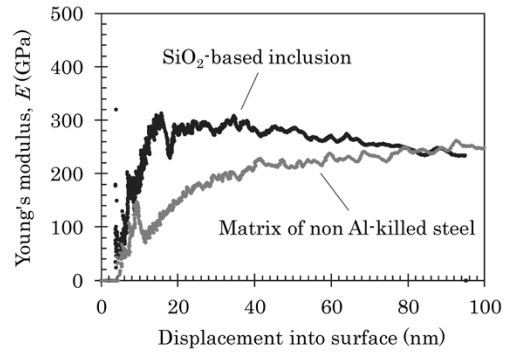


Fig. 7 Nanoindentation test result of SiO_2 -based inclusion and matrix of non Al-killed steel (Non-AL-1)

Al_2O_3 and 69 GPa for MnS.

On the other hand, the Young's modulus of the inclusions modified in the SiO_2 system (hereinafter referred to as "modified inclusions") generated in the non-Al-killed steel (Non-AL-1) is unknown, so the Young's modulus of modified inclusions was measured by the nanoindenter continuous stiffness method under the conditions of excitation vibration amplitude 2 nm and strain rate $0.05\ \text{s}^{-1}$ (Fig. 7). According to the reading of the Young's modulus in the indentation depth range where its value was relatively stable, the Young's modulus of the modified inclusions in the non-Al-killed steel was 250 to 300 GPa (indentation depth of 20 nm or more). The Young's modulus of the matrix measured simultaneously was 200 to 250 GPa (indentation depth of 40 nm or deeper) as shown in Fig. 7. That is, the ΔE of modified inclusions of the non-Al-killed steel is -100 to 0 GPa, and the absolute value of the ΔE is smaller than that of the Al_2O_3 -based inclusions observed in the Al-killed steel (AL-1).

3.5 Effect of inclusion-matrix adhesion and Young's modulus of inclusions on crack initiation

The modified inclusions in the non-Al-killed steel have greater adhesion between inclusions and matrix compared with Al_2O_3 -based inclusions generated in the Al-killed steel and have a smaller difference in Young's modulus between the matrix and inclusions. In order to investigate how these features affect the initiation of rolling contact fatigue crack with inclusions as the points of origin, the strain distribution near the inclusion under the rolling load was analyzed using the technique used by Tsuchida et al.³⁾

In the analysis, the inclusions were assumed to have a circular shape with a diameter of $20\ \mu\text{m}$, and the adhesion between the inclusion and matrix was categorized as two states: a bonded state and a flaking state. In addition, the Young's modulus of inclusions, $E_{\text{Inclusion}}$, was set to three levels: 100 GPa

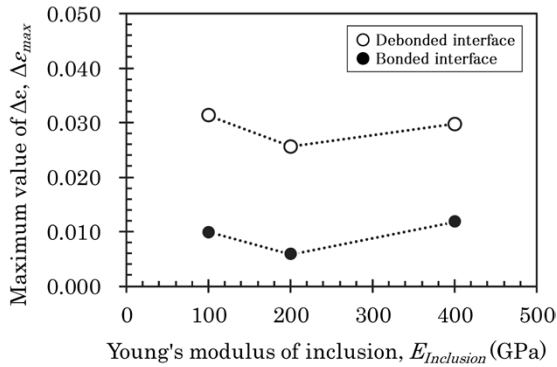


Fig. 8 Influence of interface conditions and Young's modulus of inclusions on maximum value of $\Delta\epsilon$

(simulating MnS), 200 GPa (simulating the modified inclusions in the non-Al-killed steel), and 400 GPa (simulating the Al_2O_3 -based inclusions). The crack from an inclusion as the point of origin was assumed to be initiated by mode I deformation, and from the analysis results, the change in strain, $\Delta\epsilon$, of the tensile composition in an arbitrary direction was obtained and the maximum value $\Delta\epsilon_{max}$ of $\Delta\epsilon$ was calculated.

The analysis results are shown in Fig. 8. When the inclusion-matrix adhesion is in a bonded state, $\Delta\epsilon_{max}$ is smaller in all calculating conditions (Young's modulus) than in the flaking state. Even in the case of a bonded state, it was found that $\Delta\epsilon_{max}$ takes a minimum value when Young's modulus of inclusion is close to that of the matrix (i.e., for simulated modified inclusions in the non-Al-killed steel).

In the analysis simulating Al_2O_3 -based inclusions generated in the Al-killed steel (in the flaking state, $E_{Inclusion} = 400$ GPa), $\Delta\epsilon_{max}$ is 3.0×10^{-2} , whereas, in the analysis simulating modified inclusions in the non-Al-killed steel (adhesion state, $E_{Inclusion} = 200$ GPa), $\Delta\epsilon_{max}$ decreases, becoming as small as 5.8×10^{-3} . For

this reason, cracks with inclusion as their point of origin are considered difficult to initiate from the modified inclusions of the non-Al-killed steel.

4. Mechanism of improving rolling contact fatigue life by modified oxide inclusions

The Al-killed steel had gaps between the inclusions and matrix before the fatigue test, and there was a large difference in Young's modulus between the Al_2O_3 -based inclusions and matrix. In such a case, the strain change in the tensile composition near the inclusions during rolling load increases and the initial crack with an inclusion as the point of origin is likely to be initiated.

On the other hand, the non-Al-killed steel has no gap between inclusions and matrix, which are in a bonded state. Because the difference is small between the modified inclusions in the non-Al-killed steel and the Young's modulus of the matrix, the strain change of the tensile composition near the inclusions is small. As a result, the initial cracks were suppressed, and the non-Al-killed steel was considered to have improved rolling contact fatigue properties compared with the Al-killed steel (Fig. 9).

Conclusions

Kobe Steel focused on and studied the difference in crack initiation time with the aim of elucidating the mechanism by which rolling contact fatigue properties are improved by modified oxide inclusions.

As a result, the non-Al-killed steel was found to have improved rolling contact fatigue properties compared with the Al-killed steel. The modified

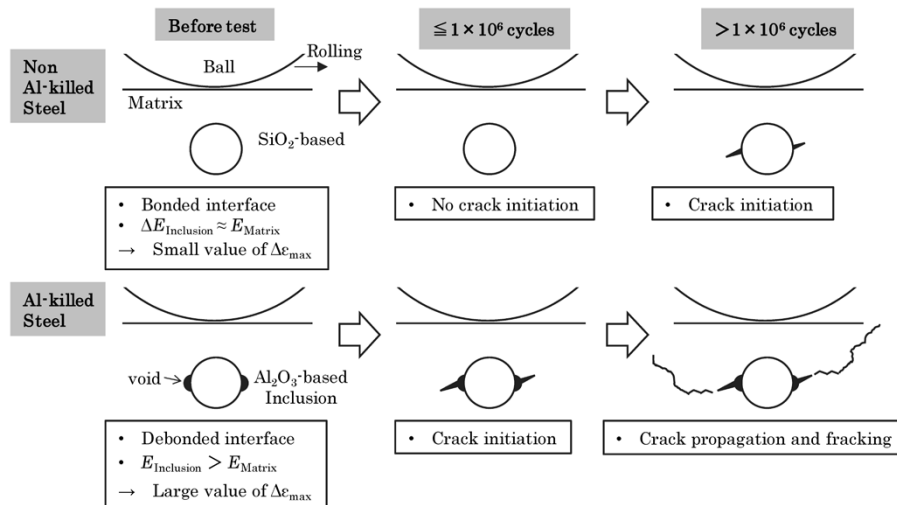


Fig. 9 Mechanism for suppressing rolling fatigue crack initiation by oxidation inclusion change

inclusions of non-Al-killed steel were found to have excellent adhesion with the matrix with a small difference in Young's modulus between the inclusions and matrix. According to the analysis, the amount of strain change that occurs near the inclusions during rolling load is reduced in the non-Al-killed steel. This was found to suppress the initial crack initiation and improve the rolling contact fatigue properties.

References

- 1) O. Umezawa. Fundamental Studies on Technologies for Steel Materials with Enhanced Strength and Functions, Proceedings of the 2nd Symposium. 2012, pp.111-112.
- 2) T. Udagawa et al. Aichi Steel technical review. 2013, Vol.30, pp.29-36.
- 3) T. Tsuchida et al. *R&D Kobe Steel Engineering Reports*. 2011, Vol.61, No.1, pp.62-65.
- 4) K. Hashimoto et al. CAMP-ISIJ. 2008, Vol.21, p.1388.
- 5) M. Shimamoto et al. ASTM Int. STP1580. 2014, pp.173-188.
- 6) A. Owaki et al. ASTM Int. STP1600. 2017, pp.487-501.
- 7) M. Ashizuka et al. Journal of the Ceramic Society of Japan. 1989, Vol.97, pp.544-548.
- 8) T. Fujimatsu et al. Tetsu-to-Hagane. 2008, Vol.94, pp.13-20.